Facilitating Robotic Subtask Reuse by a New Representation of Parametrized Solutions

Jacob P. Buch, Lars C. Sørensen, Dirk Kraft and Henrik G. Petersen
SDURobotics, The Maersk Mc-Kinney Moller Institute, University of Southern Denmark, Campusvej 55, Odense, Denmark

Keywords: Industrial Assembly Automation, Uncertainty Handling, Dynamic Simulation, Reuse of Experimental Data.

Abstract: In this paper, we suggest a coherent way of representing results from experiments associated with robotic assembly. The purpose of the representation is to be able to reuse the experiments in other assembly settings. A main novelty in our representation is the inclusion of fine grained experimental uncertainties such as e.g. deviations between a sensed object pose and the actual pose, and we discuss why it is very important for the reusability of experiments to include these uncertainties. Under the reasonable assumption that we can represent the uncertainties as a region around the origin in a potentially high dimensional Cartesian space, we show that we can efficiently represent the studied deviations by storing experiments on a so called spherical lattice. We illustrate that the representation works by studying simulation experiments on two different industrial use cases involving grasping an object and mounting an object on a fixture.

1 INTRODUCTION

Within industrial production involving assembly, there is an ever increasing demand for faster response times, smaller batch sizes and a higher degree of variation. In addition, there is a similar demand for a higher degree of automation in order to decrease cost and increase efficiency and reliability. Traditionally, assembly operations have mostly been automated by means of large static mechanical machinery with high throughput and relying heavily on strict repeatability. However, such machinery is only cost effective for very large batch sizes that are supposed to run for several or many years and are thus becoming increasingly infeasible for the above mentioned varying low volume production. Therefore, industry needs solutions that are cheap and easy to install and program and also easy to reconfigure to a new task or between different already programmed tasks.

The issue can be addressed by modularization approaches both on the mechanical and programming side. In this paper, we will purely focus on modular programming concepts. Concerning the programming issue, a common approach has been to divide overall assembly tasks into a set of “subtasks”. The idea is that solutions to subtasks can be developed for one (the first) application and reused by combining them into other applications. We adopt a wide used definition of a subtask as having a well defined interface in terms of a precondition for executing the subtask and a postcondition that the subtask is expected to produce and that can be used as precondition for the subsequent subtask. The pre- and postconditions are mostly defined at a symbolic level such as for example “objectA-in-gripper” or “objectB-detected”. The solution to the subtask is formalized as a parameterized control where the parameters are typically optimized manually for the application where the subtask is used. Together with a framework for inserting and sequencing the programmed subtasks, the overall complexity of solving a new task is strongly reduced by the modularization. The naming and precise definition of the subtasks and associated parametrized controls varies in the literature (see Section 2), but the above formulation captures the essential idea of the various approaches.

A potential problem with solving new tasks in general and also with the above approach is that it can be a slow and cumbersome process to derive the optimal (or good enough) parameters for the control. The reason for the difficulty is that there are small variations in the conditions for each execution of the task due to e.g. small random displacements of the objects. One might be able to reduce these variations mechanically and rely on strict repeatability as in traditional automation, but to reduce costs and setup times, it would be desirable to be able to select control parameters that account for these variations. In the current

Buch, J., Sørensen, L., Kraft, D. and Petersen, H.
Facilitating Robotic Subtask Reuse by a New Representation of Parametrized Solutions.
DOI: 10.5220/0005964100370048
In *Proceedings of the 13th International Conference on Informatics in Control, Automation and Robotics (ICINCO 2016) - Volume 2*, pages 37-48
ISBN: 978-989-758-198-4

state, the programmer basically teaches the program relying on a limited set of experiments using his common sense. There is no theoretical foundation for this programming activity and there is no framework for representing the generated results. Although the information (such as which control methods gave which results) from the experiments may be valuable when applying the subtask to other contexts, all this information is typically lost. In simulations or in a laboratory setting, information about the actual variation in each execution may be made available, and hence it would be desirable to derive a formulation that allows storing information on the actual variations and the outcome in a systematic and reusable way.

In this paper, we provide a theoretical formalization of teach-in programming of tasks with variations and provide a simple example that illustrates that solutions to subtasks that are programmed based on a teach-in procedure will typically rely on an insufficient set of experiments. We then suggest how to formulate a representation of experiments when we have ground truth knowledge of the variations that allows stored results to be easily reusable between different applications of the same subtask. This leads to the choice of representing executions in a systematic way, where we suggest to use a hyperspherical lattice (an equidistant multidimensional directional grid) for the variations. We then derive how such a lattice can be used to predict the outcome when executing a subtask with an arbitrary variation using interpolation techniques.

Finally, we show how we can use the method to quantitatively study the robustness of a given control to variations by an experimentally derived semi-analytical expression for the region of variations in which the execution will be successful. We study and validate the formulation using simulations with knowledge of variations of two different frequent subtasks, namely a grasping task and a placing on fixture task.

The paper is organized as follows: In Section 2, we review the state-of-the-art in more detail. In Section 3, we present the basics of our approach in terms of a mathematical formalization of executions of subtasks. In Section 4, we augment this formalization so that it becomes possible to reuse experimental results associated with optimized subtask control. This leads to the creation of a hyperspherical lattice in Section 5 for representing the impact of variations so that results can be reused between applications. In Section 6, we validate our concept based on the two different subtask examples. Section 7 concludes the paper.

2 RELATED WORK

The idea of dividing a task into subtasks with well defined interfaces is not at all new as it has been studied for decades in particular in the Artificial Intelligence community. Early work on this was on the purely symbolic side. A prominent example that has inspired much of the early work is the so called Stanford Research Institute Problem Solver (STRIPS) planner (Fikes and Nilsson, 1971). The planner uses proven components with well defined interfaces that can be combined to find a path from an initial state to a goal state. The exploitation of the concept in robotic tasks has in recent years evolved. A good example is the work by Huckaby and Christensen (Huckaby and Christensen, 2012), (Huckaby et al., 2013) which uses STRIPS for planning. Their representation of an action allows to use a SysML (System Modeling Language - an extension to UML) and a Planning Domain Definition Language to reduce the overhead for the planning of new processes. They call their subtasks “skills” these can for example be grasping, sensing or inserting. Another formulation of subtasks is presented in (Pedersen and Krüger, 2015) as a combinable function block which is also called a skill. The formulation also uses pre- and postconditions for automated sequencing. The parametrization is supposed to be provided by the user as the studied cases are rather simple.

Concerning our approach addressing reuse of obtained knowledge for assembly, the work presented in (Bjorkelund et al., 2011) is very relevant. Here, a knowledge base is developed that supports the reuse and examples within assembly are presented. However, the authors do not present a method for how the reuse is supposed to take place in general, and in particular also not how the variations should be included in the knowledge base. In (Wahrburg et al., 2015) a simpler subtask type is defined which only contains the needed components for control and coordination of a robot without any responsibility for interfaces and planning. The focus is on making the subtasks reusable by defining them as generic templates where any case specific part is extracted from parameters. Other subtask formulations can be found in e.g. (Bøgh et al., 2012), (Guerin et al., 2015).

The research on optimizing subtasks has mainly focused on one specific instance of the subtask. Much of this work is still carried out using a classical teach-in approach. For grasping great effort has been put into designing automated off-line grasp generation (Miller et al., 2003), (Vahrenkamp et al., 2011), (Bohg et al., 2014), (Rytz et al., 2015) and benchmarking of grasp solutions (Kim et al., 2013)

(Bekiroglu et al., 2011). In this process, dynamic simulation has shown to be a valuable tool. Examples like GraspIt (Miller and Allen, 2004) and OpenGrasp (Ulbrich et al., 2011) are publicly available simulators designed specifically for grasping.

A subtask where both teach-in and offline methods have been used for optimization is the peg-in-hole type insertion. In (Stemmer et al., 2006), (Stemmer et al., 2007) and (Song et al., 2014) force control based assembly strategies are proposed. They use force feedback from the robot to determine the state of the assembly subtask. In (Chhatpar and Branicky, 2005) and (Kim et al., 2012) the authors approach the problem by finding efficient search algorithms for the process and thereby the relative position uncertainty is indirectly found. Offline optimization techniques using dynamic simulation are heavily used in (Buch et al., 2014) and (Sørensen et al., 2016). An insertion trajectory is found by optimizing the relative trajectory between the peg and hole objects so that the available compliance can be optimally exploited.

3 MATHEMATICAL REPRESENTATION OF SUBTASKS WITH A FIXED APPLICATION AND A FIXED CONTROL

In this section, we first present a formulation of the execution of an arbitrary subtask as a deterministic mathematical function that maps from the detailed settings before the execution to the detailed settings after the execution. In turn, we formulate a subtask success criterion (chosen by the operator) as a binary function on the settings after the execution. We then show that deriving the control based on optimizing the success probability (using the chosen success criterion) will mostly require a very high number of executions, which calls for a representation where execution results from teach-in of one subtask can be reused for a similar subtask.

Consider a subtask as described in the introduction and recall that a subtask has a parametrized control function. When the parameters have been optimized, we shall refer to a "programmed solution" to the subtask. The subtask then comprise symbolic pre- and post-conditions and an executable program. We can view the programmed solution as a map $f : X \to Y$ described by a known function $y(x) = f(x, c(x))$, where $x \in X$ is the expected input state and $y(x) \in Y$ is the expected state after the execution. We will assume that all elements in X satisfy the precondition of the programmed solution and that X and Y can be represented as integrable subsets of (potentially high dimensional) Euclidean spaces. The state sets X and Y may thus contain fine grained information such as e.g. object poses and can have different dimensions. The function $c(x)$ denotes the programmed solution.

However, this representation is not sufficient to provide a deterministic description of a programmed solution for the subtask when variations occur. To derive a deterministic description, we should include a true state, say x_{True} in an individual execution. The true state will typically deviate from the expected state x and these deviations differ from execution to execution. The true state could for example contain the actual pose of an object as opposed to the expected state which would contain the pose computed from sensorial data. Similarly, the outcome y_{True} will deviate from the expected outcome y. As the fluctuations are unknown (otherwise they would be the expected values), we should thus view a programmed solution as an unknown function $y_{True} = f_{True}(x_{True}, c(x))$. Unfortunately, it is not possible to derive this function in the real industrial setting as both x_{True} and y_{True} will be unknown in these. We make the basic assumption that x_{True} contains the relevant data for the outcome of the execution so that the function $f_{True}(x_{True}, c(x))$ is deterministic. Furthermore, we make the reasonable assumption that $f_{True}(x, c(x)) \equiv f(x, c(x))$. In industrial settings, the programmer therefore in practice defines a success criterion for the execution, which can be measured. Formally, we can write such a success criterion as a set $S_Y(x) \subseteq Y$. Notice that although we do not y_{True}, we may know whether it is in S_Y. Consider for example a grasping task where the state y_{True} holds unknown information of the actual pose of the object relative to the gripper frame, but we can still measure whether the grasp was successful.

Assume now for simplicity that the expected state x and thus also y and S_Y are fixed. The theoretical success probability is then:

$$s = \int_X \rho(x_{True}|x)\delta_{S_Y}(f_{True}(x_{True}, c(x)))dx_{True} \qquad (1)$$

where $\rho(x_{True}|x)$ is the probability density of true states given that the expected (typically measured) state was x and $\delta_{S_Y}(y_{True})$ is one if $y_{True} \in S_Y$ and zero otherwise. This success probability can then be estimated without knowledge of $\rho(x_{True}|x)$ by simply repeating experiments with the programmed solution $c(x)$ enough times.

It should be noticed, that such a procedure to obtain an accurate estimate of s will often require many experiments. Therefore it is also difficult or impossible for the programmer to know if a programmed solution has been selected that works as desired in the long run. To see this, consider an example with ten different possible sets of control parameters of which nine has a success probability of $1-3\varepsilon$ and the last has a success probability of $1-\varepsilon$ where we assume that ε is small. Assume that we do M independent experiments with each set of control parameters. Using the Poisson approximation, we obtain that we need to carry out on the order $M = 1/\delta^2$ experiments to obtain a standard deviation that will enable us to derive the optimal programmed solution with a reasonable certainty. With $\delta = 1\%$, the operator thus need to carry out around $10,000$ experiments with each set of control parameters to be reasonable certain that the solution with the 99% success rather than 97% success has been selected. A further and more practical study on intelligent sampling methods for optimizing control parameters can be found in (Sørensen et al., 2016) where it also found that many experiments are needed.

To resolve the problem of having to perform many experiments, it would be desirable to find out how we, for an application of a subtask, can reuse the experiments with the same type of subtask carried out in different applications with different settings. An obvious difficulty with reusing programmed solutions is that there will be differences in the objects to be handled (different materials, mass density distributions, geometries etc.). This may be formally handled by a parametrization of the experimental settings through augmenting the set of expected states X. Unfortunately, there are even when disregarding these differences a couple of drawbacks when seeking to reuse the programmed solutions: i) The control was optimized with a $\rho(x_{True}|x)$ associated with the given experimental settings. In other applications, where the programmed solution is to be used, the function $\rho(x_{True}|x)$ may be significantly different and thus the control $c(x)$ may be far from optimal. A good example is grasping of a pose estimated object. The object may be picked from a table with small variations in height and tilt or from a bin with similar variations in all pose dimensions. ii) In some experiments, it may be difficult to associate a reusable success region S_Y. A good example is again grasping, where the success region S_Y for a precision grasp strongly depends on the accuracy requirements of the subsequent operation. Hence, a traditionally programmed solution (using e.g. one of the skill libraries mentioned in the related work section) is only useful for reuse if the changes in $\rho(x_{True}|x)$ and S_Y are negligible. In the next section, we will devise a representation that allow significant changes in $\rho(x_{True}|x)$ and S_Y and thus substantially increase reusability.

4 AUGMENTED SUBTASK REPRESENTATIONS FOR REUSABILITY

In this section, we augment the representation of subtask executions so that they include the true states. Clearly, the true states will not be available in the real industrial settings, but this formulation opens for the possibility of exploiting experiments performed in laboratory conditions with sensors to obtain ground truth information or (as we do in this paper) exploiting experiments carried out in computer simulations where all information of course is available. We discuss how to choose the represention and different methods for storing the results of the executions both in laboratory conditions and with computer simulations.

To deal with different $\rho(x_{True}|x)$'s and S_Y's, we need to devise a representation that is independent of these. The most direct way of achieving that is to simply study the propagation of true states relative to the expected state in a coherent way.

If we describe the propagation of true states $y_{True} = f_{True}(x_{True}, c(x))$ as $y + e_y = f_{True}(x + e_x, c(x))$, we may study the map as a propagation of errors to the expected state $e_y = \phi(e_x, c(x), x)$ where $e_x \in E_X, e_y \in E_Y$ and E_X, E_Y are small regions located around the origin in the corresponding Euclidean spaces belonging to X and Y. Notice that we assume that the map $\phi(e_x, c(x), x)$ is continuous in e_x within the region E_X. This is a reasonable assumption since we are studying potentially successful actions. We wish to derive a method that based on already performed experiments is capable of predicting the outcome of executing the programmed solution with an arbitrary error e_x without having to perform the experiment with e_x. In the simplest setting, we would wish to be able to predict whether the experiment would be successful, i.e. that $f(x + e_x, c(x)) \in S_Y$. A further step would be to be able to predict the value of $\phi(e_x, c(x), x)$. Here, we discuss two approaches that could be taken

- Random sampling in E_X together with a smoothing technique such as e.g. Kernel Density Estimation
- Interpolation in E_X using a grid (e.g. based on a hyperspherical lattice)

There are advantages and disadvantages with both approaches. The problem with random sampling is in the search phase. If the dimension of E_X is high, the total number of samples needed will also be high, and there would be a large overhead in finding the neighbors that are needed in the Kernel Density based interpolation. The disadvantage with a spherical lattice is that it requires that we can select the errors e_x. However, as we will deploy simulation for the experiments, the selection problem does not occur and we therefore choose the lattice approach. Hence, we will devise a spherical lattice that will allow instantaneous finding of the nearest lattice vectors for a given error and how these can be used to predict the error propagation $e_y = \phi(e_x, c(x), x)$.

5 CONSTRUCTION OF A SPHERICAL LATTICE

In this section, we present an algorithm for constructing a hyperspherical lattice where we adopt a method from the literature and outline how it works. A spherical lattice on a K-dimensional sphere is an organized set of approximately equidistant points on the sphere. In two dimensions these can be generated optimally by simply tesselating the unit circle into N points with angles $2\pi j/N$ for $j = 1,\dots,N$. Already in three dimensions, there are no general optimal solutions although there are special cases such as the icosahedral distribution. In higher dimensions, it become even more complicated, but several rather different methods for computing suitable lattices can be found in the literature. Here we adopt the method from (Lovisolo and da Silva, 2001) as it has the advantage of providing a lattice set that facilitates searching and also allows the user to control the grid size rather precisely. For completeness, we state the algorithm here. We first define spherical coordinates for vectors in K dimensions. If we write an arbitrary unit vector as $u = (u_1,\dots,u_K)$, a set of corresponding spherical coordinates $\theta_1,\dots,\theta_{K-1}$ can be defined as:

$$u_k = \cos\theta_k \Pi_{j=1}^{k-1} \sin\theta_j \quad k = 1\dots K-1 \tag{2}$$

$$u_K = \Pi_{j=1}^{K-1} \sin\theta_j \tag{3}$$

The user then chooses an approximate distance between neighboring lattice vectors δ and a set can then be found as follows. Choose first $\Delta\theta_1 = \delta$ and perform the tesselation $\theta_1^{(i_1)} = i_1\Delta\theta_1$. Assume now that a tesselation has been derived for spherical coordinate $k-1$ and consider an arbitrary point of that tesselation $(\theta_1^{(i_1)}, \theta_2^{(i_2)}, \dots, \theta_{k-1}^{(i_{k-1})}$. We can then compute the size of the tesselation of the spherical coordinate k by computing:

$$\Delta\theta_k = \frac{\delta}{\Pi_{j=1}^{k-1} \sin\theta_j^{(i_j)}} \tag{4}$$

and subsequently choose $\theta_k^{(i_k)} = i_k\Delta\theta_k$. Notice that for $k > 1$, we thus have a variable $\Delta\theta_k$ selected so that the distance between adjacent points will be δ. Due to boundaries on the spherical coordinate, the lattice will not be perfect, but we have tested it to be useful even for a rather small size of the lattice. Moreover, the choice of δ should be rather intuitive for the user.

6 USING THE SPHERICAL LATTICE TO APPROXIMATE THE ERROR TRANSFORMATIONS AND SUCCESS REGIONS USING SIMULATIONS

We now study a subtask using simulation. For any input error e_x, the simulator thus produces a resulting error $e_y = \phi(e_x, c(x), x)$, and we wish to estimate this map using our spherical lattice.

Lattice Data Generation: The first step is to choose an appropriate scaling (choice of unit) for each of the coordinates of e_x so that we can select the same maximal error distance D for all directions (and thus for all lattice vectors) that we wish to sample. For each lattice vector, say u_k, we select a tesselation ε of error points along the vector u_k where we perform simulations. The next step is thus to perform simulations with errors $s_{ik} = i\varepsilon u_k$ for each lattice vector and for $i = 1,\dots,\lceil \frac{D}{\varepsilon} \rceil$. We record the deterministic outcomes $\sigma_{ik} = \phi(s_{ik}, c(x))$ generated by executing the simulation.

Prediction: Consider now an arbitrary error e_x. We then search for the K nearest lattice vectors that correspond to the corners in the $K-1$ dimensional hyperplane on the surface of the unit sphere to which e_x belongs. To do this efficiently, we may compute the spherical coordinates of e_x and use the structure of the lattice to obtain the hyperplane with a rather limited search. We then select the nearest tesselation point relative to the size of e_x and perform a weighted linear interpolation between these to obtain an estimate of $\phi(e_x, c(x), x)$.

We are thus immediately able to use this for various studies such as to estimate the overall success probability of the programmed solution $c(x)$ for any $\rho(x_{True}|x)$ and any S_Y by noticing that we can write (1) as:

$$s = \int_X \rho(x + e_x|x)\delta_{S_Y}(f_{True}(x + e_x, c(x)))de_x \tag{5}$$

and deploying a classical sample point based numerical integration schemes.

In this paper, we wish to illustrate the validity of our method in a simple way by studying the success regions directly. To determine the success region, we for each lattice vector, say u_k, compute the largest distance d_k where all errors αu_k belong to the success region when $\alpha \leq d_k$. If all values up to Du_k belongs to the success region, we set $d_k = D$.

For an arbitrary error vector e_x, we then again search for the K nearest lattice vectors that corresponds to the corners in the $K-1$ dimensional hyperplane on the surface of the unit sphere to which e_x belongs. We can then provide a conservative estimate by testing if e_x is closer to the origin than the scaled hyperplane with corners $d_k s_k$ for the relevant $K-1$ lattice vectors.

7 VALIDATING OUR CONCEPTS ON TWO SUBTASKS

In this section, we test our concept on two subtasks. The first subtask consist of grasping of an industrial object using a Robotiq two fingered hand and the second case is the placement of the same object into a fixture. For each subtask, three types of errors and associated success regions are studied where each handles a specific type of uncertainty. The first error type includes the positional uncertainties of an object placed on a table. The second includes errors in all three positional dimensions to illustrate the concept for any positional uncertainties. Lastly, a full six-dimensional error illustrates any transformational uncertainty for an object.

For each of the cases, we compare the actual outcome (success/failure) with the predicted outcome computed as outlined in the end of the previous section. By this, we will study the value of using the derived representation for a detailed robustness of a given control to uncertainties.

7.1 Grasping of Industrial Object Subtask

In the grasping subtask, an industrial part is grasped by a Robotiq two fingered gripper. The length of the industrial part is $5\,cm$ and has a diameter of $3\,cm$ where it is largest. The scene is shown in Figure 1. The grasping strategy starts by the hand being placed $10\,cm$ above the grasping location and it is then moved linearly down to the grasping location. At this position, the gripper is set to close, and finally, the hand is again lifted to the initial position. At this point, the simulation is evaluated. In the evaluation, it is tested whether the object is still in contact with both the fingers. If so, the action is evaluated as a success and

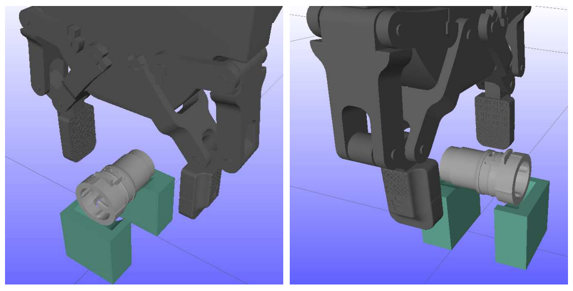
Figure 1: Scene for the grasping subtask. It consists of a fixed fixture, a dynamic industrial object and a kinematically controlled Robotiq hand with dynamically controlled fingers.

otherwise as a failure.

The dynamic simulation engine chosen for this task is the Open Dynamics Engine (Drumwright et al., 2010), which is a widely used engine in the robot community and has in particular been used for grasping. The engine is interfaced using RobWork(Ellekilde and Jorgensen, 2010). In the engine, the friction between the fingers and the industrial object was set to $\mu = 0.9$. The robotic hand was modeled as individual bodies for each finger part connected by joints. The finger is then driven by a torque added between the base and the first outermost finger part which is used to pull the fingers together when grasping the object. The object is picked from a simple fixture comprised of a box with a small cut out to hold it in place. Contacts between fixture and gripper are ignored in simulation.

7.1.1 2D Positional Errors when Grasping Objects from a Table

The industrial part is, in this case, perturbed in the directions of a plane to simulate the errors which could occur if the object was placed on a table, i.e. $e_x \in \mathbb{R}^2$. The area is estimated by two different sets of lattice vectors with respectively six and twelve vectors. The search vector is maximally evaluated up to $D = 12\,cm$ and the used tesselation is $\varepsilon = 1\,mm$. The success areas are illustrated in Figure 2, together with 4000 random perturbations generated from a realistic distribution. The distribution chosen was a two-dimensional normal distribution with mean $0\,cm$ and standard deviation $\sigma = 8\,cm$ in both directions and with no correlation. Qualitatively, the plot shows that the region is very well captured with these two rather sparse lattices. Typically, the success area will grow in size when refining the lattice as the polyhedral shortcuts will be smaller, which can also be seen in the Figure. However, in the first quadrant, the success area of the 12 lattice vector case is smaller than the 6 lattice case

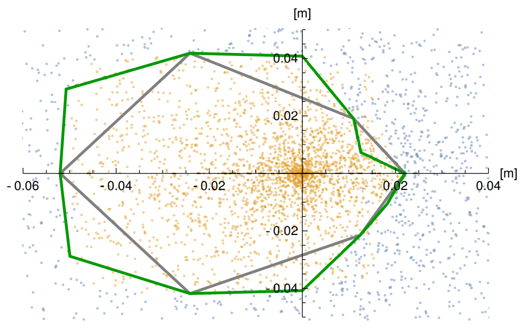

Figure 2: 2D success areas of the grasping action and 4000 perturbations taken from a two dimensional normal distribution with mean 0 cm and standard deviation 9 cm in both dimensions. Blue dots indicate a failure while yellow indcate a success. The six search vector based success area is illustrated in black and the twelve search vector based success area is illustrated in green.

due to what seems to be a simulation artifact.

For quantification, the performance is for all our experiments measured with a confusion matrix and a histogram. The histogram shows the distribution of the four results from the confusion matrix with respect to the distance to the boundary of the estimated success region. Points inside the region have negative distances in the histogram.

For the 2D case, the results are illustrated for the coarse lattice with six vectors in Figure 3. The confusion matrix illustrates a very good estimation where 92 % of the experiments were correctly estimated with respect to the success area and only 0.57 % are a critical false positive. False positives are more critical since they can result in unexpected failures whereas false negatives just represent a too strict success area. Notice also from the histogram that all of the false estimates are close to the edge of the success area.

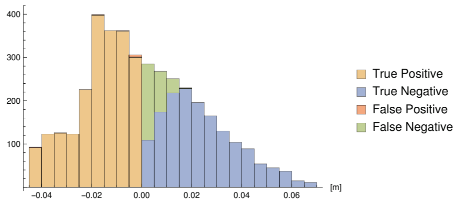

		Predicted		
		Success	Failure	Total
Executed in simulation	Success	2111	305	2416
	Failure	9	1575	1584
	Total	2120	1880	4000

Figure 3: Histogram and confusion matrix for the 2D positional errors based on six lattice vectors for the grasping subtask.

For the twelve vectors based success area, the results are shown in Figure 4. Despite the artifact in the first quadrant, this success area has a better coverage of the real success area where 96 % of all perturbations were correctly estimated. It has as expected a small increase to 1.5% in the critical false-positive percentage due to the more tight estimation of the success region.

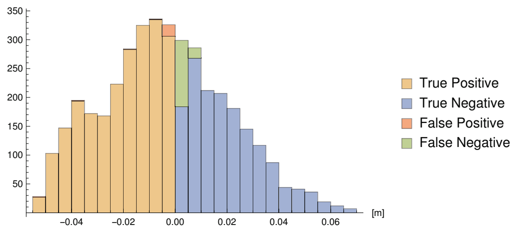

		Predicted		
		Success	Failure	Total
Executed in simulation	Success	2283	133	2416
	Failure	24	1560	1584
	Total	2307	1693	4000

Figure 4: Histogram and confusion matrix for the 2D positional errors based on twelve lattice vectors for the grasping subtask.

7.1.2 3D Positional Errors when Grasping an Object

In the second experiment, we also include the third positional dimension, i.e. $e_x \in \mathbb{R}^3$. To estimate the success area, we again consider two lattices based respectively on 12 and 42 vectors. As it is difficult to illustrate plots of the regions in more than two dimensions, we have chosen to omit these. The performance can however again be estimated by a confusion matrix and a histogram. We again used 4000 perturbations, but now taken from a three-dimensional normal distribution with identical standard deviation of $\sigma = 8\,cm$ in each dimension. The results with twelve lattice vectors are shown in Figure 5.

The performance is not quite as good as for the two-dimensional success area, but still more than 90% are correctly estimated and still only less than 2% of the critical false positive are present in both cases. The performance for the success region based on 42 vectors is shown in Figure 6. The results in the confusion matrix has again an increase in false positives due to the tighter fit, but has a larger decrease in false negatives and thus an overall better representation of the success region.

7.1.3 6D Errors for Grasping an Object

We now consider grasping objects with pose errors in all six dimensions (three in position and three in orientation). A success area is best represented by

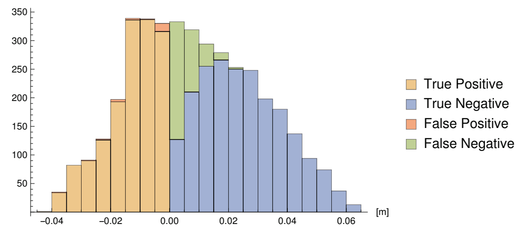

		Predicted		
		Success	Failure	Total
Executed in simulation	Success	1515	370	1885
	Failure	26	2089	2115
	Total	1541	2459	4000

Figure 5: Histogram and confusion matrix for the 3D positional errors based on 12 lattice vectors for the grasping subtask.

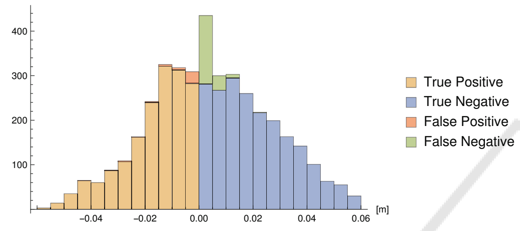

		Predicted		
		Success	Failure	Total
Executed in simulation	Success	1689	196	1885
	Failure	42	2073	2115
	Total	1731	2269	4000

Figure 6: Histogram and confusion matrix for the 3D positional errors based on 42 lattice vectors for the grasping subtask.

the lattice vectors if there is an equivalence between translation and rotation. To ensure this, we have chosen a relation of the units to be so that $1\,cm$ is equivalent to $0.3\,rad$ roughly corresponding to an object of a size of $5-10\,cm$. The success region is estimated with lattices of respectively respectively 98 and 1004 lattice vectors corresponding to $\delta = 0.8$ and $\delta = 0.5$. The performance is again studied using 4000 perturbations, which is now taken from a distribution with a standard deviation of $5\,cm$ in the three positional dimensions and $\sigma = 1\,rad$ in roll, pitch and yaw.

The results for the success region estimated from 98 search vectors is illustrated in Figure 7. There is a now a rather significant set of 43.75 % of the actually successful perturbations that are falsely predicted as a false negative. This indicates that the conservative success region estimate obtained from cutting off with the polyhedral shortcuts now has an impact.

The results with 1004 lattice vectors are illustrated in Figure 8. We see that the estimate is improved over the 98 based six-dimensional success area, but there are still many successful tests that were predicted as

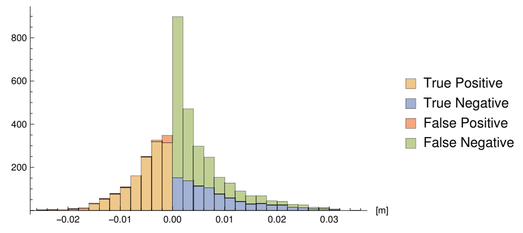

		Predicted		
		Success	Failure	Total
Executed in simulation	Success	1333	1750	3083
	Failure	68	849	917
	Total	1401	2599	4000

Figure 7: Histogram and confusion matrix for the 6D errors based on 98 lattice vectors for the grasping subtask.

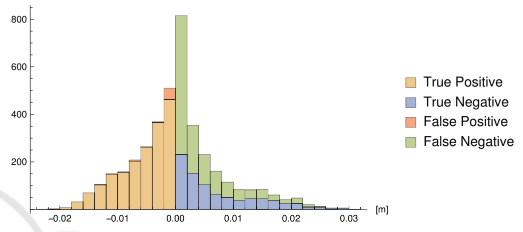

		Predicted		
		Success	Failure	Total
Executed in simulation	Success	1811	1272	3083
	Failure	64	853	917
	Total	1875	2125	4000

Figure 8: Histogram and confusion matrix for the 6D errors based on 1004 lattice vectors for the grasping subtask.

failure. For both cases, we however observe around 7 % of the failures were now false positives.

7.2 Placing in Fixture Subtask

The second investigated subtask is a placement of the same industrial part into a fixture. The scene is shown in Figure 9 and consist of two elements. A compliant fixture and an industrial part which is kinematically controlled. The compliance in the fixture is modeled by fixing the body to the world with a damped spring. The spring has a directional compliance which is set to $0.0005\,m/N$, the rotational compliance is set to $0.1\,\frac{1}{N\cdot m}$ and the friction is chosen so the system is critically damped. The control used with the insertion to simply place the object linearly from above. The industrial object is initially held $15\,cm$ above the targeted final position in the fixture. From that position, the object is moved directly downwards to the final position. The simulation is then evaluated at simulation end time. For evaluation, we examine the tip of the fixture. If the tip of the fixture is at least $1\,cm$ inside the industrial part the simulation is evaluated as

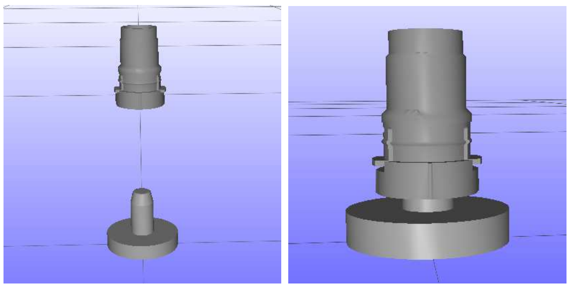
Figure 9: Scene for the place in fixture case. The left image shows the initial position and the right image the goal position of the subtask.

a success, otherwise it is a failure.

Since this action is a tight fit insertion, we found based on recent studies (Thulesen and Petersen, 2016) that ODE was not suitable to simulate the task. Based on these studies, *anonomous* was chosen to accurately simulate tight-fit assembly. We used the standard settings of the engine except for the friction coefficient, which was set to 0.4 corresponding to interactions between two plastic objects. We again study $2D$ and $3D$ positional errors and the $6D$ general error with the same lattices as for the grasping subtask.

7.2.1 2D Positional Errors for Placing an Object on a Fixture

The results for the estimation of the success region were again obtained with 4000 perturbations and a plot is shown in Figure 10. The perturbations are here again taken from a two-dimensional normal distribution but with a lower standard deviation $\sigma = 2.5cm$ since this action is much less resilient to uncertainties.

The quantitative results are again shown with confusion matrices and histograms and are illustrated in

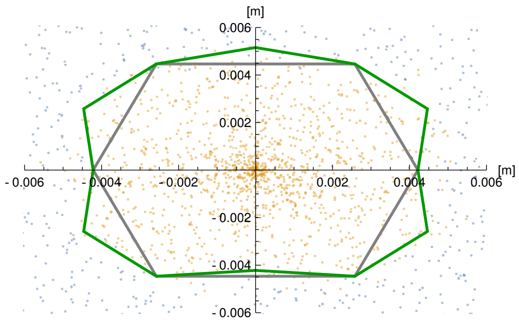

Figure 10: 2D success areas of the place in fixture action and 4000 perturbations taken from a two dimensional normal distribution with mean $0cm$ and standard deviation $2.5cm$ in both dimensions. Blue dots indicate a failure while yellow indcate a success. The six search vector based success area is illustrated in black and the twelve search vector based success area is illustrated in green.

Figure 11 and Figure 12 respectively. The results show that both success regions are very well estimated with only a few false classifications and the performance looks very similar to the corresponding results from the grasping action.

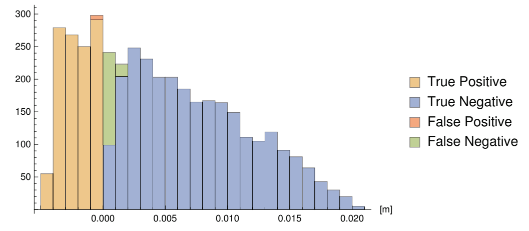

		Predicted		
		Success	Failure	Total
Executed in simulation	Success	1143	161	1304
	Failure	7	2689	2696
	Total	1150	2850	4000

Figure 11: Histogram and confusion matrix of 2D success area estimated based on six search vectors for the place in fixture subtask.

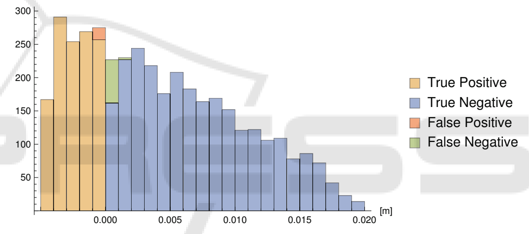

		Predicted		
		Success	Failure	Total
Executed in simulation	Success	1238	68	1306
	Failure	18	2676	2694
	Total	1256	2744	4000

Figure 12: Histogram and confusion matrix of 2D success area estimated based on twelve search vectors for the place in fixture subtask.

7.2.2 3D Positional Errors for Placing an Object on a Fixture

This study is similar to the study for the success region for the three-dimensional grasping case, but with the perturbations are taken from a distribution with standard deviation of $\sigma = 2.5cm$ in all three dimensions. The results is shown in Figure 13 and Figure 14.

Again the quality of matching is similar to the grasping subtask with only around 0.5% false positives, but here there is a somewhat surprising improvement on the false negatives by going to 42 lattice vectors.

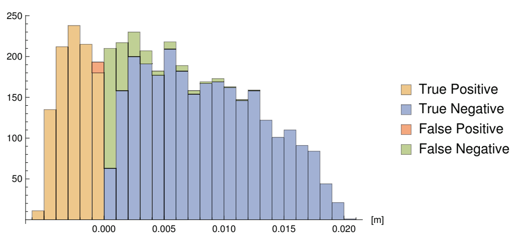

		Predicted		
		Success	Failure	Total
Executed in simulation	Success	991	286	1276
	Failure	13	2710	2723
	Total	1004	2996	4000

Figure 13: Histogram and confusion matrix of 3D success area estimated based on twelve search vectors for the place in fixture subtask.

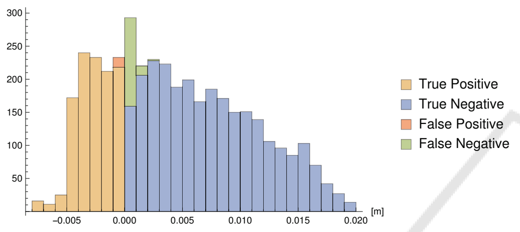

		Predicted		
		Success	Failure	Total
Executed in simulation	Success	1127	150	1277
	Failure	15	2708	2723
	Total	1142	2858	4000

Figure 14: Histogram and confusion matrix of 3D success area estimated based on 42 search vectors for the place in fixture subtask.

7.2.3 6D Errors for Placing an Object on a Fixture

For this subtask, the last experiments also considers all six dimensions of pose errors. The perturbations are taken from a distribution with standard deviation of $\sigma = 2\,cm$ in the position and $\sigma = 0.6\,rad$ in roll, pitch and yaw. The performance of the success area is shown in Figure 15 and Figure 16 for the success area created from 98 search vectors and 1004 search vectors respectively. Again, we obtain results that are quite similar to those for the grasping subtask with around 7% false positives.

8 CONCLUSION

In this paper, we have outlined how to represent outcomes of experiments when uncertainties are available to be used in frameworks where robotic tasks are divided into subtask components that are aimed at be-

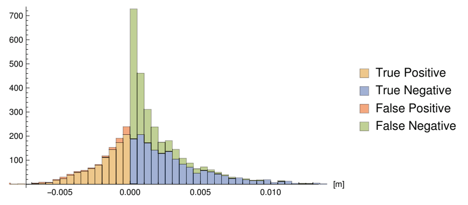

		Predicted		
		Success	Failure	Total
Executed in simulation	Success	979	1275	2254
	Failure	116	1630	1746
	Total	1095	2905	4000

Figure 15: Histogram and confusion matrix for the 6D errors based on 98 lattice vectors for the place in fixture subtask.

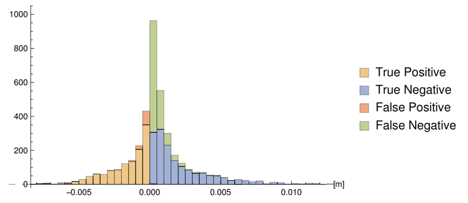

		Predicted		
		Success	Failure	Total
Executed in simulation	Success	1224	1030	2254
	Failure	125	1621	1746
	Total	1349	2651	4000

Figure 16: Histogram and confusion matrix for the 6D errors based on 1004 lattice vectors for the place in fixture subtask.

ing reused. We have discussed why it is important to include uncertainties and that classical teach-in approaches rely on two main flaws, namely that there will often be too few experiments for obtaining the optimal solution and that reuse in different settings is problematic. We then show how our suggested representation can resolve this issue. Our method relies on sampling with ground truth knowledge of the uncertainties. These conditions can be met in simulation as shown by our experiments or by executing the tasks in laboratory conditions where the uncertainties can be measured.

It is clear from our tests that the quality of our estimates of the success area seems to decrease with increase in the dimensionality of the state space. A main reason for this is that the amount of necessary grid points in the hyperspherical lattice grows exponentially with the dimension of the uncertainty space. Hence, when we use the grid for directly estimating $\phi(e_x, c(x), x)$, we will study how to develop a grid that at the different locations on the hypersphere adapts the grid size to a required accuracy of the interpolation. In the near future, we will also conduct studies of reusing the representation between different but similar subtasks. Furthermore, we want to use the representation to estimate $\rho(x_{True}|x)$ for a full task as a tool to estimate the optimal control parameters for each of the subtasks constituting the full task.

REFERENCES

Bekiroglu, Y., Laaksonen, J., Jorgensen, J. A., Kyrki, V., and Kragic, D. (2011). Assessing grasp stability based on learning and haptic data. *Robotics, IEEE Transactions on*, 27(3):616–629.

Bjorkelund, A., Edstrom, L., Haage, M., Malec, J., Nilsson, K., Nugues, P., Robertz, S., Storkle, D., Blomdell, A., Johansson, R., Linderoth, M., Nilsson, A., Robertsson, A., Stolt, A., and Bruyninckx, H. (2011). On the integration of skilled robot motions for productivity in manufacturing. In *Assembly and Manufacturing (ISAM), 2011 IEEE International Symposium on*, pages 1–9.

Bøgh, S., Nielsen, O. S., Pedersen, M. R., Krüger, V., and Madsen, O. (2012). Does your robot have skills? In *Proceedings of the 43rd International Symposium on Robotics (ISR2012)*.

Bohg, J., Morales, A., Asfour, T., and Kragic, D. (2014). Data-driven grasp synthesis - a survey. *Robotics, IEEE Transactions on*, 30(2):289–309.

Buch, J. P., Laursen, J. S., Sørensen, L. C., Ellekilde, L.-P., Kraft, D., Schultz, U. P., and Petersen, H. G. (2014). Applying simulation and a domain-specific language for an adaptive action library. In *Lecture Notes in Computer Science*, volume 8810, pages 86–97.

Chhatpar, S. and Branicky, M. (2005). Particle filtering for localization in robotic assemblies with position uncertainty. In *Intelligent Robots and Systems, 2005. (IROS 2005). 2005 IEEE/RSJ International Conference on*, pages 3610–3617.

Drumwright, E., Hsu, J., Koenig, N., and Shell, D. (2010). Extending open dynamics engine for robotics simulation. *Second International Conference, SIMPAR 2010, Darmstadt, Germany*, (3):38–50.

Ellekilde, L.-P. and Jorgensen, J. A. (2010). Robwork: A flexible toolbox for robotics research and education. pages 1 –7.

Fikes, R. E. and Nilsson, N. J. (1971). Strips: A new approach to the application of theorem proving to problem solving. In *Proceedings of the 2Nd International Joint Conference on Artificial Intelligence*, IJCAI'71, pages 608–620, San Francisco, CA, USA. Morgan Kaufmann Publishers Inc.

Guerin, K. R., Lea, C., Paxton, C., and Hager, G. D. (2015). A framework for end-user instruction of a robot assistant for manufacturing. In *Robotics and Automation (ICRA), 2015 IEEE International Conference on*, pages 6167–6174.

Huckaby, J. and Christensen, H. (2012). A taxonomic framework for task modeling and knowledge transfer in manufacturing robotics. In *Proc. 26th AAAI Cognitive Robotics Workshop*, pages 94–101.

Huckaby, J., Vassos, S., and Christensen, H. (2013). Planning with a task modeling framework in manufacturing robotics. In *Intelligent Robots and Systems (IROS), 2013 IEEE/RSJ International Conference on*, pages 5787–5794.

Kim, J., Iwamoto, K., Kuffner, J., Ota, Y., and Pollard, N. (2013). Physically based grasp quality evaluation under pose uncertainty. *Robotics, IEEE Transactions on*, 29(6):1424–1439.

Kim, Y.-L., Kim, B.-S., and Song, J.-B. (2012). Hole detection algorithm for square peg-in-hole using force-based shape recognition. In *Automation Science and Engineering (CASE), 2012 IEEE International Conference on*, pages 1074–1079.

Lovisolo, L. and da Silva, E. A. B. (2001). Uniform distribution of points on a hyper-sphere with applications to vector bit-plane encoding. *IEE Proceedings - Vision, Image and Signal Processing*, 148(3):187–193.

Miller, A. and Allen, P. (2004). Graspit! a versatile simulator for robotic grasping. *Robotics Automation Magazine, IEEE*, 11(4):110–122.

Miller, A., Knoop, S., Christensen, H., and Allen, P. (2003). Automatic grasp planning using shape primitives. In *Robotics and Automation, 2003. Proceedings. ICRA '03. IEEE International Conference on*, volume 2, pages 1824–1829 vol.2.

Pedersen, M. R. and Krüger, V. (2015). Automated planning of industrial logistics on a skill-equipped robot. In *IROS 2015 workshop Task Planning for Intelligent Robots in Service and Manufacturing, Hamburg, Germany*.

Rytz, J. A., Ellekilde, L., Kraft, D., Petersen, H. G., and Krüger, N. (2015). On transferability and contexts when using simulated grasp databases. *Robotica*, 33(5):1131–1146.

Song, H.-C., Kim, Y.-L., and Song, J.-B. (2014). Automated guidance of peg-in-hole assembly tasks for complex-shaped parts. In *Intelligent Robots and Systems (IROS 2014), 2014 IEEE/RSJ International Conference on*, pages 4517–4522.

Sørensen, L. C., Buch, J. P., Petersen, H. G., and Kraft, D. (2016). Online action learning using kernel density estimation for quick discovery of good parameters for peg in hole insertion. In *13th International Conference on Informatics in Control, Automation and Robotics (ICINCO)*. To be submitted.

Stemmer, A., Albu-Schaffer, A., and Hirzinger, G. (2007). An analytical method for the planning of robust assembly tasks of complex shaped planar parts. In *Robotics and Automation, 2007 IEEE International Conference on*, pages 317–323.

Stemmer, A., Schreiber, G., Arbter, K., and Albu-Schaffer, A. (2006). Robust assembly of complex shaped planar parts using vision and force. In *Multisensor Fusion and Integration for Intelligent Systems, 2006 IEEE International Conference on*, pages 493–500.

Thulesen, T. N. and Petersen, H. G. (2016). RobWork-PhysicsEngine: A new dynamic simulation engine for manipulation actions. In *Robotics and Automation (ICRA), 2016 IEEE International Conference on*. (accepted).

Ulbrich, S., Kappler, D., Asfour, T., Vahrenkamp, N., Bierbaum, A., Przybylski, M., and Dillmann, R. (2011). The opengrasp benchmarking suite: An environment for the comparative analysis of grasping and dexterous manipulation. In *Intelligent Robots and Systems (IROS), 2011 IEEE/RSJ International Conference on*, pages 1761–1767.

Vahrenkamp, N., Przybylski, M., Asfour, T., and Dillmann, R. (2011). Bimanual grasp planning. In *Humanoid Robots (Humanoids), 2011 11th IEEE-RAS International Conference on*, pages 493–499.

Wahrburg, A., Zeiss, S., Matthias, B., Peters, J., and Ding, H. (2015). Combined pose-wrench and state machine representation for modeling robotic assembly skills. In *Proceedings of the IEEE/RSJ Conference on Intelligent Robots and Systems*, pages 852–857.